

See discussions, stats, and author profiles for this publication at: <https://www.researchgate.net/publication/262112105>

# Ammonia Photodissociation Promoted by Si(100)

ARTICLE *in* THE JOURNAL OF PHYSICAL CHEMISTRY A · MAY 2014

Impact Factor: 2.69 · DOI: 10.1021/jp408543e · Source: PubMed

---

CITATIONS

2

---

READS

33

2 AUTHORS, INCLUDING:



[Anthony J. Muscat](#)

The University of Arizona

57 PUBLICATIONS 669 CITATIONS

SEE PROFILE

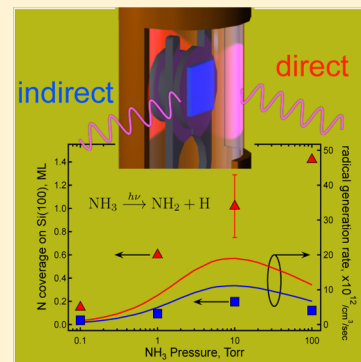
# Ammonia Photodissociation Promoted by Si(100)

Casey C. Finstad and Anthony J. Muscat\*

Department of Chemical &amp; Environmental Engineering University of Arizona Tucson, Arizona 85721, United States

## S Supporting Information

**ABSTRACT:** Using in situ X-ray photoelectron spectroscopy measurements after reaction, we show that hydrogen-terminated Si(100) perturbs the bonding of physisorbed  $\text{NH}_3$  enabling a photochemical decomposition pathway at wavelengths different from those characteristic of either the molecule in the gas phase or the semiconductor bandgap. UV illumination only of gas phase  $\text{NH}_3$  at partial pressures from 0.1 to 100 Torr produced a maximum at 10 Torr in the N surface coverage. This is in good agreement with a model of the radical production rate showing that at this pressure the gas density balances the flux of photons at the surface with energies sufficient to dissociate  $\text{NH}_3$ . UV illumination of both the gas phase and the surface produced a monotonic increase in the N coverage with pressure as well as coverages that were 3–10 times higher than when only the gas phase was illuminated. The amine saturation coverage scaled with the UV fluence at 10 Torr and 75 °C, reaching  $6.9 \times 10^{14}$  atoms/cm<sup>2</sup> ( $\sim 1$  N atom per Si surface atom) at 19 mW/cm<sup>2</sup> and  $12 \times 10^{14}$  atoms/cm<sup>2</sup> ( $\sim 1.8$  N per Si) at 35 mW/cm<sup>2</sup>. Monochromatic illumination showed that the wavelengths driving deposition were not correlated with the Si bandgap, but instead were roughly the same as gas phase photodissociation ( $\lambda < 220$  nm). The primary driving force to replace the hydrogen termination with amine groups was direct photodissociation of  $\text{NH}_3$  molecules whose electronic structure was perturbed by interaction with the surface. Amine groups enhanced the surface reaction of water present as a contaminant in the source gas. These results show that molecules in weakly bound surface states can have a dramatic impact on the photochemistry.



## INTRODUCTION

Electronic excitations in molecules and on surfaces can drive nonthermal chemical reactions that selectively promote one product among all of the possibilities. On a semiconductor surface, this often means stopping a gas–surface reaction at an intermediate state relative to the thermally driven reaction sequence. One example is the use of ultraviolet (UV) light to break dichlorine  $\text{Cl}_2$  into atoms that replace the hydrogen termination on Si(100) at low temperature.<sup>1,2</sup> Si surfaces can be chlorinated via thermal activation, but the high temperature also desorbs silicon chlorides, etching the surface. The lowest energy electronic transitions for molecules are driven by the absorption of visible to ultraviolet photons having energies up to a few electronvolts, whereas on semiconductor surfaces the energies needed to generate hot carriers are typically lower. When molecules in the gas phase are put in contact with a surface and irradiated by light, photons can be directly absorbed by the gas phase molecules, by the substrate, and by the molecules adsorbed on the surface of the substrate. Each of these pathways could be acting alone or in parallel. Techniques that delineate between these possible excitation paths can quantify the relative contribution that each makes. Once identified, the specific excitation pathway may be utilized as a new synthetic route for semiconductor interfaces that are important in a host of applications.

The techniques used to distinguish between direct absorption and surface-mediated mechanisms are key topics in any discussion of surface photochemical reactions, and the determination of the mechanism or mechanisms at work

provides insight into how specific photochemical pathways can be selectively promoted. One common method of distinguishing between different pathways is simply to measure the response to variations in the photon energy. Gluck et al.<sup>3</sup> investigated the photodecomposition of mono- and multilayers of physisorbed  $\text{Mo}(\text{CO})_6$ ,  $\text{W}(\text{CO})_6$ , and  $\text{Fe}(\text{CO})_5$  on Si(111) at 90 K under 257 and 514 nm illumination. A direct absorption mechanism was confirmed by the observed decomposition of the carbonyls at 257 nm, which falls within the absorbance spectrum of all three molecules, but no observed reaction at 514 nm, which exceeds the Si bandgap energy but is outside the carbonyl absorbance spectrum. If photoexcited carriers within the Si were responsible, the authors concluded that decomposition would have been observed at both wavelengths.

Zhu et al.<sup>4</sup> investigated UV irradiation of chemisorbed  $\text{NH}_3$  at 102 K to activate the growth of nitride passivation layers on GaAs(100) surfaces. Because photolysis occurred even at wavelengths too long for direct  $\text{NH}_3$  absorption, they concluded that substrate-mediated photogenerated electrons were primarily responsible. By analyzing the postexposure surfaces with X-ray photoelectron spectroscopy (XPS), high resolution electron energy loss spectroscopy (HREELS), and temperature-programmed desorption (TPD), they determined that the decomposition of  $\text{NH}_3$  resulted in  $\text{NH}_2$  groups on the

Received: August 26, 2013

Revised: May 5, 2014

Published: May 6, 2014

surface, which decomposed until the surface was saturated with GaN. Arsenic nitrides formed as well but were lost due to their higher volatility. Zhu et al. also used time-of-flight mass spectroscopy (TOF-MS) to show that photoinduced desorption occurred at all wavelengths with a photon energy greater than the GaAs bandgap (1.43 eV). Unlike photodissociation, a marked increase in the photodesorption cross-section was observed at 193 nm (6.4 eV), which is within the  $\text{NH}_3$  absorption envelope. This indicates that photodesorption was significantly enhanced by direct absorption of photons by adsorbed molecules (surface-localized photodissociation), which occurred in parallel with the substrate-mediated mechanism.<sup>5</sup> Similar experiments with  $\text{PH}_3$  and  $\text{AsH}_3$  on GaAs(100) showed that the likelihood of the adsorbate photodissociating rather than photodesorbing was strongly influenced by the surface–adsorbate bond.<sup>6</sup>

The substrate can play a significant role in maintaining the population of precursor molecules, as illustrated by the photochemistry of condensed films. Direct participation in photolysis and more subtle effects that depend on the strength of the chemical interaction between the adsorbate and the surface are possible.<sup>7</sup> Interaction with a substrate perturbs the bonding of a molecule, even when it is weakly bound. Depending on the extent of stabilization the surface provides the initial and final electronic states of the molecule, the perturbation can shift molecular transitions, and therefore the absorbance spectrum, by 0.1–1 eV relative to the gas phase spectrum.<sup>8</sup> Chakarov and Ho quantified this effect for  $\text{H}_2\text{S}$  chemisorbed on Si(111) at 69 K.<sup>9</sup> Using electron energy loss (EEL) spectroscopy to probe the electronic transitions of  $\text{H}_2\text{S}$ , they found that the primary peak shifted by 0.65 eV to the red, which is roughly equivalent to a shift from 193 to 215 nm. At coverages of 0.25–0.5 monolayer (ML),  $\text{H}_2\text{S}$  photodissociated with a wavelength dependence matching that of Si(111). As the coverage increased to 1.25 ML, a new photodissociation mechanism with a wavelength dependence characteristic of direct photon absorption dominated. The photodissociation cross-section for this higher coverage mechanism followed the gas phase absorbance spectrum but was, like the EEL spectrum, red-shifted by 0.65 eV. As explained by Chakarov and Ho, a red-shifted spectrum indicates a decreased energy difference between the ground and excited states. If the interaction between the substrate and adsorbate stabilizes the excited state, the energy difference decreases and the spectrum red shifts. If the substrate primarily stabilizes the ground state, the energy difference increases causing the spectrum to blue shift. Chen and Osgood<sup>10</sup> also observed a red shift of the absorbance spectrum upon adsorption of  $\text{Cd}(\text{CH}_3)_2$  on fused silica. They also noted broadening and dampening of the vibrational components of the spectrum.

The gas phase photolysis of  $\text{NH}_3$  by UV light has been well studied.<sup>11–14</sup> Even though 280 nm photons have the same energy as a N–H bond, the photons are not absorbed by  $\text{NH}_3$  and do not drive photochemical reactions. It is only at wavelengths shorter than 220 nm that photons are absorbed, promoting the  $\text{A}(^1\text{A}_2'') \leftarrow \text{X}(^1\text{A}_1')$  transition and leading to scission of the N–H bond.<sup>11</sup> The strong vibrational band structure results in a spectrum consisting of a series of strong absorption lines spaced at 3–4 nm intervals, of which line broadening causes the tails to overlap into a broad continuum centered at 194 nm.<sup>15</sup> The ground state of  $\text{NH}_3$  is a trigonal pyramid, but all excited states are planar. Once created, the

excited state can quickly ( $<50$  fs)<sup>16</sup> decompose through two different pathways:<sup>11</sup>



At 206 nm (6.03 eV), pathway 1 occurs with a quantum efficiency of nearly one, whereas pathway 2 occurs with only 0.5% efficiency.

On a bare, reconstructed Si(100)-2×1 surface,  $\text{NH}_3$  will readily adsorb dissociatively across a dimer, adding a dihydride amine to one silicon dimer atom and a H atom to the other, saturating at 0.5 ML of amine with all remaining Si atoms terminated by hydrogen.<sup>17–19</sup> After saturation of the bare Si(100)-2×1 surface, or on initially H-terminated Si, the surface is reactive toward  $\text{NH}_3$  only above 430 °C, when H desorbs. For this reason, silicon nitridation is usually done at temperatures well above 430 °C, to drive hydrogen desorption and maintain a population of dangling bonds on the surface.<sup>20</sup> Also in this temperature range (300–400 °C), surface amine groups begin to lose hydrogen atoms and incorporate into the substrate.<sup>21–25</sup> The primary amine incorporates itself into an adjacent Si–Si bond to form a secondary amine (Si–NH–Si) and, ultimately, incorporates into an additional adjacent bond to form a tertiary amine, eventually forming a stoichiometric  $\text{Si}_3\text{N}_4$  film.

Nonthermal photoactivation of  $\text{NH}_3$  has been described for low temperature silicon nitride growth. Bater, Sanders, and Craig<sup>26</sup> adsorbed  $\text{NH}_3$  on Si(100) at 110 K, and then irradiated the surface with an electron beam (150 eV, 120  $\mu\text{A}/\text{cm}^2$ ) for 30 min to convert all adsorbed  $\text{NH}_3$  to nitride. At currents of 1  $\text{mA}/\text{cm}^2$  and an  $\text{NH}_3$  ambient of  $6 \times 10^{-8}$  Torr, a nitride growth rate of 1 Å/min was achieved. Cerrina et al.<sup>27</sup> exposed Si(111) surfaces to  $\text{NH}_3$  at room temperature and then exposed the surfaces with the adsorbed  $\text{NH}_3$  to the full spectrum output from a synchrotron. Soft X-ray photoelectron spectroscopy showed the formation of Si–N bonds after the synchrotron exposure. Sugii, Ito, and Ishikawa<sup>28</sup> exposed H-terminated Si(100) to a UV laser (195 nm, 40 mJ/pulse) under an  $\text{NH}_3$  ambient at 400 °C, and grew silicon nitride layers that saturated at 25 Å after 2000 pulses. They concluded their film was comparable to one grown thermally at 700 °C. Watanabe et al.<sup>29</sup> used Xe flash lamps to drive nitridation of Si(100) under pure  $\text{NH}_3$ . At 260 °C, their nitride layer saturated at about 3.5 ML. They concluded it was a thermally activated process because they believed their lamps lacked output in the wavelengths necessary to photodissociate  $\text{NH}_3$ . It is possible that they underestimated the output of their lamps at wavelengths below 220 nm and actually observed a photon-enhanced process similar to the one reported here. As described above for GaAs(100), Zhu et al. used a pulsed UV laser (193 and 248 nm) to activate physisorbed  $\text{NH}_3$  to grow a passivating surface nitride.<sup>4</sup> Nonthermal activation was necessary to prevent desorption of volatile arsenic nitride compounds. In addition to gallium and arsenic nitride groups, the UV activation also resulted in the formation of primary amine ( $-\text{NH}_2$ ) surface groups. To deliberately leave the amines as surface terminating groups instead of growing a silicon nitride, chlorine has been used to replace the hydrogen termination on silicon, chemically activating the surface and lowering the activation energy required to react  $\text{NH}_3$  with

Si(100).<sup>1</sup> This pathway did not yield full monolayer coverage and left residual Cl.

Amine terminated Si has recently been identified as a potential starting surface for interfaces between Si and dielectric layers.<sup>25,30,31</sup> Investigations of HfO<sub>2</sub> by atomic layer deposition (ALD) on Si has shown that deliberate incorporation of N at the Si/HfO<sub>2</sub> interface impedes the formation of interfacial silicon oxide that would otherwise spontaneously form during thermal processing.<sup>32,33</sup> The interfacial oxide has a lower dielectric constant and, if it forms, reduces the overall capacitance of the metal-oxide-semiconductor (MOS) transistor, decreasing the switching speed. Bulk nitride layers have low thermal expansion coefficients and the nitrogen atom has a moderate electronegativity, is small, and typically is 3-fold coordinate. These properties may be useful in the rational design of interfaces in devices that employ semiconductors. The amine surface is also effective for attaching copper phthalocyanine<sup>34</sup> and glycine<sup>35</sup> to Si substrates. Phthalocyanine complexes are useful in organic optoelectronic devices, and a glycine terminated silicon surface will have improved biocompatibility properties for inorganic implants.

Herein, we describe the photochemical deposition of amine groups at low temperature (25–150 °C) and moderate pressure (0.1–100 Torr) on liquid-cleaned Si(100). The amine coverage increased with time and illumination intensity, eventually saturating. The N deposition rate peaked at 10 Torr when the surface was indirectly illuminated, consistent with model predictions due to depletion of UV photons by gas phase absorption, whereas the rate increased monotonically with pressure when the surface was directly illuminated. Using monochromatic light, we show that N deposition correlates with the ammonia absorption envelope and not with electron–hole pair creation at the surface. We propose that physisorption of NH<sub>3</sub> on the top layer of atoms terminating the Si surface slightly shifted the optical absorption spectrum of the molecules to wavelengths different from those characteristic of the gas phase.

## ■ EXPERIMENTAL SECTION

Experiments were performed in an apparatus consisting of multiple reaction chambers connected to a surface analysis chamber by a high vacuum transfer tube.<sup>36</sup> This allowed surfaces to be processed and analyzed in situ with XPS (Physical Electronics 549, double-pass cylindrical mirror analyzer, 200 eV pass energy, 300 W Al anode X-ray source), without exposure of the samples to the ambient. Surface coverage was estimated using XPS and a quantitative calibration curve that was generated from a copper film sputtered in situ onto a silicon substrate. Published sensitivity factors specifically for surface species<sup>37</sup> were used to adapt the calibration curve for other elements. All non-Si atoms were assumed to be on the surface, even when total coverages exceeded one monolayer. The published sensitivity factor for each element is an average of measurements made on multiple compounds. The precision in these values was not reported, but the coverages are probably accurate to within 25% based on visual inspection of the raw data.<sup>37</sup>

N<sub>2</sub> (from liquid boil off) and NH<sub>3</sub> (Scott Specialty Gases, Electronic grade, 99.999%) gas were metered into an externally heated quartz tube reactor (GE grade 214, 35 mm i.d., 30 cm long) illuminated by UV light from an external 1000 W Xe arc lamp (Spectral Energy Corporation, LH 151N).<sup>1,36</sup> The light entered horizontally into the vertically oriented tube. The

sample was held on a manipulator whose axis of rotation was concentric with the reactor tube and contained by the plane of the sample holder. This allowed the orientation of the sample with respect to the illumination beam to be changed without affecting either the distance between the center of the sample, where XPS measurements were taken, and the light source or the flow dynamics of the gas in the axial direction. When focused for maximum intensity, the lamp illuminated the sample with a flux of 35 mW/cm<sup>2</sup>, as measured by a radiometer with a 6 mm diameter window. When desired, fluence was decreased by adjusting the collimating lens to provide more diffuse light with a larger spot size. For the samples processed at the lowest illumination levels, a screen was used to partially block the light beam. The fluence values reported are suitable for qualitative comparisons but the accuracy of the radiometer calibration was not verified.

An infrared filter limited unintended sample heating to <3 K, as measured by a thermocouple mounted between the sample and the stainless steel sample holder during temperature calibration. The sample temperature was reproduced to ±5 K using a resistive heater wrapped around the tube and thermostatically controlled using a thermocouple mounted on the reactor wall, external to the vacuum. A calibration curve was measured with only N<sub>2</sub> flowing to relate the thermostat setting to the actual sample temperature. Illumination had no effect on the measured temperature. The entire reactor was shrouded to eliminate external light and to fully contain the UV illumination, and the shroud was purged with N<sub>2</sub> to prevent O<sub>3</sub> formation. A monochromator (Jarrell-Ash Monospec 27, 240 nm blaze) was inserted between the lamp and reactor when needed for wavelength resolved studies.

Silicon (100) samples (p type, 38–63 Ω·cm) were cut into 1.5 × 2 cm<sup>2</sup> pieces and cleaned using a repeated sequence of dilute HF (1:100 49% HF:ultrapure water, 5 min) and piranha solution (5:1 H<sub>2</sub>SO<sub>4</sub>:30% H<sub>2</sub>O<sub>2</sub>, 5 min) liquid cleans, using each bath twice and then ending with a 10 min dilute HF bath to leave the surface H-terminated with a minimal concentration of O ((1.2 ± 0.3) × 10<sup>14</sup> atoms/cm<sup>2</sup>), C ((1.7 ± 0.3) × 10<sup>14</sup> atoms/cm<sup>2</sup>), and F ((0.3 ± 0.1) × 10<sup>14</sup> atoms/cm<sup>2</sup>). [Caution: Piranha solution is aggressive and explosive. Never mix piranha waste with solvents. Check the safety precautions before using it.] The errors define 95% margins of error based on sample-to-sample variation calculated for all samples. Si samples were mounted on holders that could be readily transferred between the UV reactor and surface analysis chamber. NH<sub>3</sub> was exposed to the sample as a mixture of 10% NH<sub>3</sub> in N<sub>2</sub>. The NH<sub>3</sub> partial pressure was used as a set point and ranged from 0.1 to 100 Torr (0.013–13 kPa). Sample temperatures of 25–150 °C were studied. All calculations assumed an ideal gas, and molecular flux values were estimated using the kinetic theory of gases,<sup>38</sup> neglecting the inert N<sub>2</sub>. A turbo pump returned the reactor to high vacuum (10<sup>−7</sup> Torr) conditions for sample transfer.

## ■ RESULTS

Exposing an H-terminated Si surface at 75 °C to NH<sub>3</sub> gas (10% NH<sub>3</sub> in N<sub>2</sub> at a total pressure of 100 Torr produced an NH<sub>3</sub> flux of 4.5 × 10<sup>21</sup> molecules/(cm<sup>2</sup>·s) for 10 min did not deposit N based on the XPS spectrum (Figure 1a), but when illuminated by a 35 mW/cm<sup>2</sup> output from the Xe arc lamp, 4.3 × 10<sup>14</sup> N atoms/cm<sup>2</sup> were added to the sample, as indicated by the presence of the N 1s peak at 398.7 eV<sup>1,39</sup> (Figure 1b). If the Si(100) surface atom density is 6.78 × 10<sup>14</sup> atoms/cm<sup>2</sup>, this



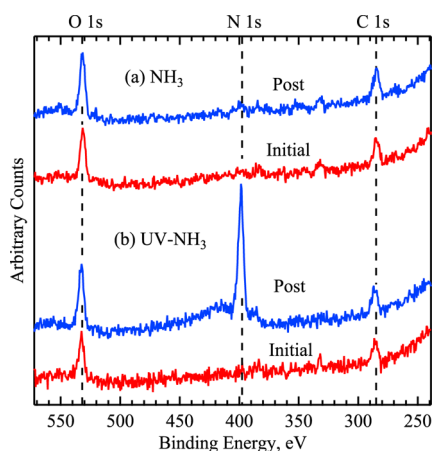


**Figure 1.** XPS spectra showing two H-terminated Si(100) samples before and after exposure to 10 Torr  $\text{NH}_3$  at 75 °C, for 10 min. (a) Under dark conditions, no reaction was observed, but (b) with UV illumination ( $35 \text{ mW}/\text{cm}^2$ ),  $4.3 \times 10^{14}$  N atoms/ $\text{cm}^2$  were deposited and the coverage of O increased by  $1.4 \times 10^{14}$  atoms/ $\text{cm}^2$ .

corresponds to 0.64 nitrogen containing amine groups per surface Si atom, i.e., 0.64 ML of amine groups. Peaks corresponding to the O 1s state at 532.8 eV and the C 1s state at 286.2 eV were also present. Increasing the illumination intensity increased the N deposition rate. Figure 2 shows that the N coverage monotonically increased with the UV flux for 20 min exposures of an  $\text{NH}_3$  gas flux of  $4.5 \times 10^{21}$  molecules/ $(\text{cm}^2 \cdot \text{s})$ .

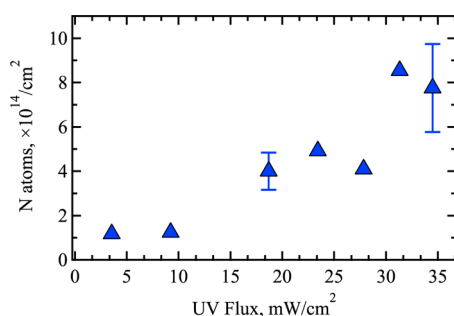


**Figure 2.** N coverage on H-terminated Si(100) as a function of UV flux for 20 min exposures with 10 Torr  $\text{NH}_3$  at 75 °C. The intensity was altered by inserting filter screens into the light path (below  $10 \text{ mW}/\text{cm}^2$ ) and by focusing the beam (above  $20 \text{ mW}/\text{cm}^2$ ). The  $\text{NH}_3$  flux was constant at  $4.5 \times 10^{21}$  molecules/ $(\text{cm}^2 \cdot \text{s})$ . The error bars show 95% confidence intervals for multiple samples processed with the same UV flux.

Figure 3 shows the increase in the N coverage with time at two different UV illumination levels. The coverage increased and eventually reached saturation. Because the UV flux was controlled by adjusting the focus of the light beam, it was more difficult to maintain uniform illumination under high UV flux conditions, increasing the error. Interestingly, the coverage at saturation depended on the UV flux used for the deposition: with illumination at  $19 \text{ mW}/\text{cm}^2$ , the N coverage ( $\theta_{\text{N, sat}}$ ) saturated at  $6.9 \times 10^{14}$  atoms/ $\text{cm}^2$  (1.0 ML), and with the UV illumination at  $35 \text{ mW}/\text{cm}^2$ ,  $\theta_{\text{N, sat}}$  increased proportionally to  $12 \times 10^{14}$  atoms/ $\text{cm}^2$  (1.8 ML). Select samples were analyzed by AFM for surface roughness and averaged  $1.66 \pm 0.14 \text{ \AA}$  (rms), which was comparable to the  $1.61 \pm 0.18 \text{ \AA}$  measured on

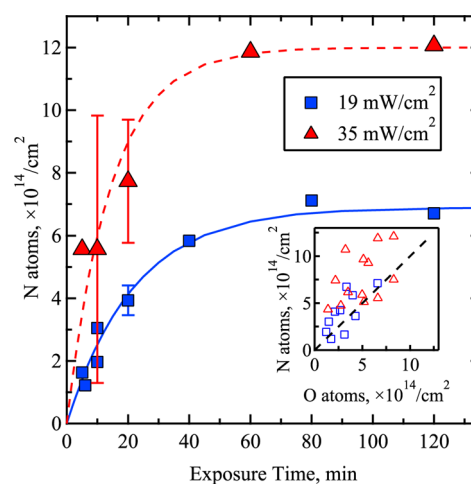


**Figure 3.** N coverage as a function of time for H-terminated Si(100) exposed to 10 Torr  $\text{NH}_3$  at 75 °C for two different UV fluxes. The lines are of the form  $\theta_{\text{N}} = \theta_{\text{N, sat}}(1 - \exp(-\alpha_{\Phi}t))$  where values of  $\alpha_{\Phi}$  were found by least-squares fits to be  $0.046 \text{ min}^{-1}$  at  $19 \text{ mW}/\text{cm}^2$  and  $0.69 \text{ min}^{-1}$  at  $35 \text{ mW}/\text{cm}^2$ . The inset shows that the final O coverage generally increased with N at a rate of roughly one O atom for every 2 N atoms. The error bars represent 95% margins of error computed from multiple data points; the wide error bars on the high illumination intensity data are the result of focusing the light beam, which decreased the spatial uniformity of the illumination.

untreated samples. There was no trend in surface roughness with respect to processing time or UV flux.

The N (amine) terminated surfaces were highly reactive toward the water contamination in the source gas, resulting in oxidation. At higher UV fluxes, the nitridation rate increased, resulting in an increased initial deposition rate (slope at time zero, Figure 3). The oxidation rate was not catalyzed by the illumination, so N was better able to compete with O for the limited number of reaction sites, resulting in the higher value for  $\theta_{\text{N, sat}}$  observed in Figure 3 for  $35 \text{ mW}/\text{cm}^2$ . The O coverage was generally proportional to the N coverage, as shown in the inset of Figure 3. The initial O coverage was typically  $(1.2 \pm 0.3) \times 10^{14}$  O atoms/ $\text{cm}^2$ , on the basis of XPS measurements of the starting H-terminated surface, and increased at a rate of approximately one O atom for every two N atoms added based on a least-squares fit to the data shown in the inset of Figure 3.

The initial H-terminated surface was unreactive toward the  $\text{H}_2\text{O}$  present in the reaction chamber, whether at base pressure or with the reactive gas present. It was only when the combination of UV and  $\text{NH}_3$  was used to deposit N (amine groups) that the O signal began to increase. The source  $\text{NH}_3$  gas had a specified maximum  $\text{H}_2\text{O}$  content of 5 ppm ( $5 \times 10^{-6}$  Torr  $\text{H}_2\text{O}$  when the  $\text{NH}_3$  partial pressure was set to 10 Torr) and was previously identified as the source of water contamination in the reactor.<sup>1</sup> Amine-terminated samples were left at base pressure for days with no measurable change in the XPS spectrum. An amine-terminated sample left in the cleanroom ambient for 28 h showed an increasing O coverage at approximately four times the rate at which an H-terminated control sample oxidized, as determined by periodic XPS measurements (data not shown). As the O coverage increased, the N coverage simultaneously decreased with approximately three O atoms added for each N atom lost.

The rate of  $\text{NH}_3$  photolysis varied with pressure and UV flux, but not temperature (Figure 4). Although the N coverage at 25

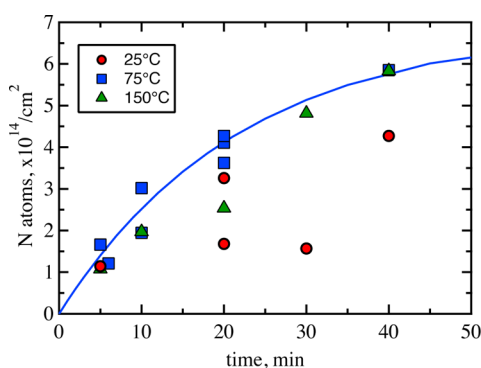


**Figure 4.** N coverage on H-terminated Si(100) as a function of temperature for a flux of 19 mW/cm<sup>2</sup> with 10 Torr NH<sub>3</sub>. The solid blue line is the same blue curve plotted in Figure 3 for 19 mW/cm<sup>2</sup> UV flux at 75 °C.

°C is generally lower than at the other two temperatures over the range of deposition times up to 40 min, there is a lot of scatter in the data. This combined with the similarity in the N coverages at 75 and 150 °C, leads us to conclude that the temperature dependence of the N coverage is weak. The UV intensity was attenuated (screened) by NH<sub>3</sub>, so the rate of NH<sub>2</sub><sup>•</sup> radical production decreased exponentially with the distance the photons traveled after entering the reactor. To understand how the reactor geometry and pressure affected the reaction conditions, a model was used to predict the NH<sub>2</sub><sup>•</sup> radical production rates within the reactor that accounted for the spectral distribution of the light source, attenuation by the optics and reactor wall, and the gas phase absorption of NH<sub>3</sub> (details in the Supporting Information). Assuming a quantum efficiency of one, the model yields the radical generation rate as a function of position along the centerline of the light beam between the quartz reactor wall and the sample. The rate reaches a maximum in the vicinity of the sample at an NH<sub>3</sub> partial pressure of 10 Torr for both indirect and direct illumination of the substrate (dotted and solid lines in Figure 5). Below this pressure, the radical generation rate increased because there were more molecules available for dissociation, and above this pressure the rate decreased due to the screening of the relevant photons by NH<sub>3</sub> in the gas phase. Experimental results for the indirect illumination configuration follow the same trend with respect to pressure, showing maximum N deposition at 10 Torr (blue squares in Figure 5). Under direct illumination, however, there was no maximum. The N coverage increased monotonically with increasing pressure, resulting in  $9.6 \times 10^{14}$  N atoms/cm<sup>2</sup> deposited in 20 min when the NH<sub>3</sub> partial pressure was increased to 100 Torr. The resulting N coverage was 3–10 times higher using direct illumination for NH<sub>3</sub> pressures of 0.1–100 Torr.

To gain insight into the reaction mechanism, samples were processed using light filtered by a monochromator to determine how the system behavior was affected by the illumination wavelength. Figure 6 shows the wavelength-dependent amine incorporation rate (red triangles) superimposed on top of the gas-phase absorption spectrum for NH<sub>3</sub> (solid green line). Figure 6 also shows the calculated spectrum of available photons (dashed purple line) and the absorption spectrum for the silicon substrate (black dotted line). As explained in the Supporting Information, these two spectra were used to estimate the electron–hole pair creation rate (solid blue line) and predict the wavelength-dependent relative reaction rate for

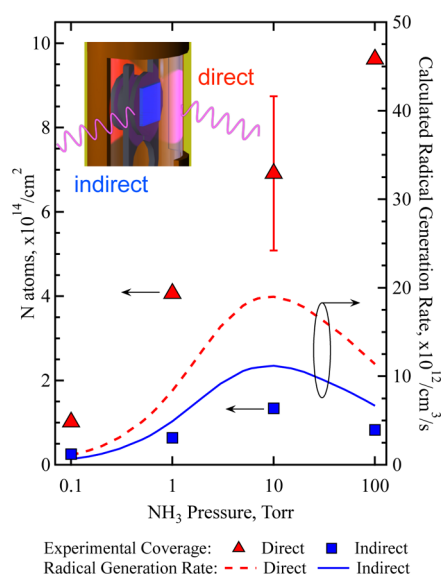


**Figure 5.** Effect of increasing NH<sub>3</sub> pressure on N coverage for 20 min exposures (75 °C, 35 mW/cm<sup>2</sup> UV illumination). The red triangles (left axis) show direct (normal) illumination data and the blue squares (left axis) indirect illumination (light rays parallel to surface) data. The lines (right axis) show the NH<sub>2</sub><sup>•</sup> production rates for direct (dashed) and indirect (solid) illumination that were calculated using eqs S1 and S3 (Supporting Information) at the center of the reactor where the sample surface was located.

a surface-mediated reaction mechanism. The coverages deposited using monochromatic radiation were only ~10% of the coverages deposited without the monochromator due to the decreased photon flux, but as illustrated in Figure 6, the deposition mechanism became more active as the photon wavelength decreased from 260 nm (4.7 eV) to 190 nm (6.5 eV); the results show the actual coverage achieved and were not normalized by photon flux. NH<sub>3</sub> absorbs light below 220 nm (5.6 eV), within the window where the monochromatic deposition results show the most dramatic increase, between 225 nm (5.5 eV) and 212 nm (5.8 eV). There was a small but measurable amount of surface amine groups deposited using monochromatic exposures centered at 225 and 230 nm, but this was attributed to the wide bandwidth of the monochromator (11 nm fwhm). Even when the monochromator output was centered on 230 nm, there would have been a finite number of sub-220 nm photons allowed to pass.

## DISCUSSION

At temperatures below 400 °C, NH<sub>3</sub> does not react with H-terminated Si. To deposit N, UV photons must initiate the reaction by converting NH<sub>3</sub> into the more reactive NH<sub>2</sub><sup>•</sup>. Because deposition occurred only when the photon energy overlapped with the absorbance spectrum (Figure 6), the activation energy was provided by the absorption of UV photons by NH<sub>3</sub>. The results for the indirect illumination geometry in Figure 5 show that activating the NH<sub>3</sub> in the gas phase produced NH<sub>2</sub><sup>•</sup> radicals that diffused to the Si surface and reacted, depositing N. Activating the gas phase alone yielded a maximum radical generation rate (calculated, solid blue line) and maximum N deposition rate (experimental, blue squares) at 10 Torr of NH<sub>3</sub> when the temperature was maintained at 75 °C. At lower pressures there were more photons available with sufficient energy than NH<sub>3</sub> molecules to

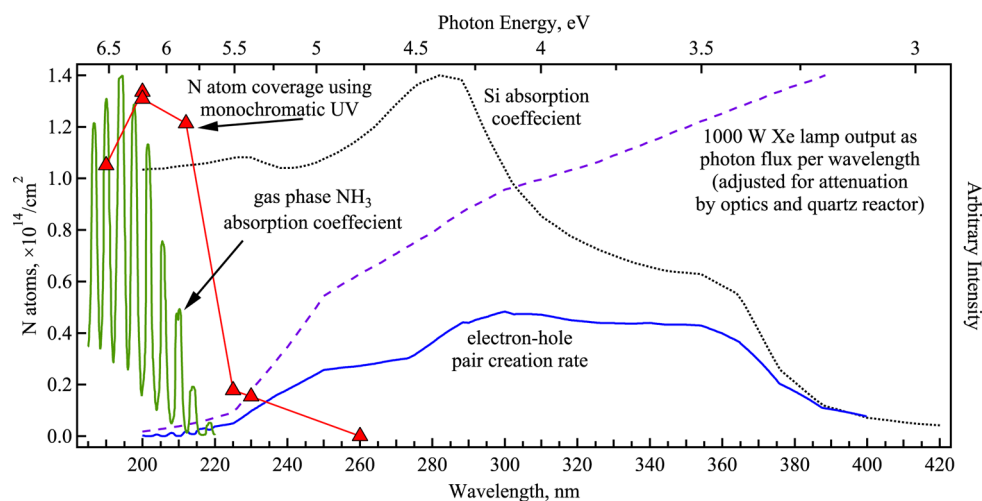


**Figure 6.** N coverage on H-terminated Si(100) as a function of wavelength for samples exposed to monochromatic (11 nm fwhm) UV photons for 40 min at 75 °C, under 10 Torr  $\text{NH}_3$  (red triangles). The deposition results are overlaid on the absorbance spectra of gas phase  $\text{NH}_3$ <sup>11</sup> (green line) and crystalline  $\text{Si}^{40}$  (dotted black line), as well as the output spectrum for the Xe lamp corrected for absorbance by the optics and quartz reactor (dashed purple line). The solid blue line gives the wavelength-dependent surface electron–hole pair generation rate, estimated using a model developed by Ying and Ho<sup>41</sup> (see eq S4, Supporting Information).

dissociate, and at higher pressures the relevant photons were increasingly absorbed by the gas molecules closer to the light source, hindering  $\text{NH}_2^\bullet$  radical generation at the center of the reactor where the sample was located. The photon blocking effect was a function of both the  $\text{NH}_3$  density and the reactor geometry. According to the model, the maximum radical generation rate shifts toward higher pressures as the temperature increases or the length of the light path through the  $\text{NH}_3$  gas decreases.

In the direct illumination geometry, 20 min exposures resulted in N coverages that were 3 to 10 times higher than those obtained at the same pressure in the indirect configuration. The coverage increased monotonically as  $\text{NH}_3$  pressure increased from 0.1 to 100 Torr, rather than going through a maximum as the model predicted and as observed in the indirect illumination experiments. The reactor was designed to keep the light path constant whether the illumination was provided directly or indirectly, and the cylindrical symmetry of the reactor ensured that the axial gas flow dynamics were the same for either sample orientation, so the concentration of gas phase radicals should be similar with respect to the measurement location in both configurations. One effect that was not controlled for experimentally but was included in the calculations was the increased photon density due to reflection by the polished Si sample. Reflection only increased the photon density by  $\sim 70\%$ <sup>42</sup> and cannot completely account for the observed increase in amine deposition. If the deposition reaction is first order with respect to the  $\text{NH}_2^\bullet$  radical concentration, as expected, then the deposition rate would be roughly 70% higher. Even if the deposition reaction is second order in the  $\text{NH}_2^\bullet$  radical concentration, the deposition rate would increase by almost 3 times, not enough to explain the 10 times increase observed at 100 Torr. If gas phase absorption of the activating photons cannot explain the deposition behavior with direct illumination, then there must be an additional surface–adsorbate or surface–photon interaction by which the surface enhanced the deposition reaction.

At 10 Torr, the indirect configuration resulted in only 16% as many surface amines as the direct configuration for 20 min exposures, implying 16% of the observed coverage in the direct

configuration was the result of photoactivation of gas phase molecules and 84% of the coverage was the result of a surface influenced enhancement. The monochromatic experiments were done in the direct illumination geometry and so primarily give the wavelength dependence of the surface enhancement. If the enhancement was the result of a surface mediated mechanism, then the wavelength dependence of the deposition rate should have mirrored the  $r_{e-h}$  curve (solid blue line) in Figure 6, which predicts a maximum at roughly 300 nm—a lower photon energy than the 200 nm maximum observed experimentally. The  $r_{e-h}$  curve reflects the wavelength-dependent rate that photoexcited carriers are generated, but it is not an indication of the electron energy. Even under monochromatic illumination, electrons are effectively produced in a continuum of energies<sup>43</sup> that range from the maximum possible, when the electron is excited out of the top of the valence band and experiences no inelastic collisions before encountering the adsorbate, all the way down to zero energy, either because the electron has dissipated all of its energy by inelastic collisions and phonon scattering, or because the initial state of the electrons was lower in energy than the top of the valence band and therefore required more energy to reach an excited state. The effect of this is that as long as the photon energy exceeds the energy threshold required to generate a photoexcited electron with energy resonant to a specific transition, then there will be a population of resonant electrons available. Because the electron may have to overcome a potential barrier or possess a minimum energy for resonant attachment, it is possible that the monochromatic illumination results would also show a threshold—below the threshold no reaction would be observed, but above the threshold the reaction rate would follow the shape of the  $r_{e-h}$  curve. The experimental results did show a threshold wavelength below which there was no deposition, but once that threshold was exceeded, there was no correlation between the experimental monochromatic results in Figure 6 and the  $r_{e-h}$  curve, implying the reaction mechanism does not involve the resonant attachment of photoexcited electrons to adsorbed  $\text{NH}_3$  molecules. In the Supporting Information, we argue further that an excited electron from the substrate into a



resonant state on  $\text{NH}_3$  is not possible at the wavelengths available.

The HOMO of  $\text{NH}_3$  is 5–6 eV below the valence band edge of Si (Figure S1, Supporting Information). Because only direct illumination of the surface monotonically increased the N coverage, the hole states that are present in the p-type material at equilibrium do not play a significant role in ammonia dissociation. If photogenerated holes contributed, then the process requires two photons: one to generate a hot hole and another to excite an electron from the  $\text{NH}_3$  HOMO to the hole state. We discount multiphoton excitation events due to the low flux of photons used in this work. Under full illumination, the photon flux at all wavelengths shorter than 1107 nm (1.12 eV, band gap of Si) is estimated to be  $\sim 10^{17}$  photons/( $\text{cm}^2 \cdot \text{s}$ ), or roughly 7 ms to absorb one photon per surface atom. This is longer than the typical minority carrier lifetime in Si (2.5 ms).<sup>44</sup> Furthermore, the monochromatic experiments used several orders of magnitude fewer photons and would have shown a significantly lower yield if multiphoton interactions were necessary.

The wavelength dependence of the N coverage that we observed is the same as for direct activation of the gas phase. Only exposures using wavelengths shorter than 220 nm resulted in significant N deposition. Photodecomposition pathways and products are not necessarily the same for surface and gas phase processes involving the same reactant.<sup>3</sup> But the similar energies required for the two processes strongly suggests that both mechanisms involve the same electronic states on the same species. The Ho group<sup>3,41</sup> observed a similar phenomenon with the photoinduced decomposition of saturated monolayer coverages of  $\text{Mo}(\text{CO})_6$  molecularly adsorbed on Si(111) at 90 K—there was no reaction at wavelengths longer than 360 nm, but when shorter wavelengths were used, CO desorbed from the surface. The absorbance spectrum of  $\text{Mo}(\text{CO})_6$  starts at 355 nm and increases to its first maximum at 290 nm.<sup>45</sup> Because the excitation mechanism for the  $\text{Mo}(\text{CO})_6$  adsorbed on the surface required the same photon energy as the vapor, they concluded the excitation mechanism involved direct photon absorption by the physisorbed molecules.

The results in Figure 5 show that the photoexcitation of  $\text{NH}_3$  molecules associated with the surface was promoted over the gas phase process. This yielded the linear increase in N coverage with  $\text{NH}_3$  pressure despite photon screening. We reconcile the effect of a covered Si surface with direct excitation of  $\text{NH}_3$  by looking more closely at the  $\text{NH}_3$  absorption spectrum. The spectrum consists of vibrational bands of intense absorption spaced roughly 4 nm apart superimposed on a broad background. For wavelengths at which  $\text{NH}_3$  is strongly absorbing (peaks in the absorbance spectrum), few photons are available for reaction at the Si surface, but at wavelengths where  $\text{NH}_3$  is weakly absorbing (valleys in the absorbance spectrum) photons are available to drive the reaction. For example, at 201.5 nm, more than 99.9% of the initial photons were absorbed by the gas phase before reaching the Si (Figure 7). But at 204 nm, 50% of the photons entering the reactor reach the sample surface, but are less likely to result in gas phase  $\text{NH}_3$  photolysis due to the smaller cross-section. If physisorption of the  $\text{NH}_3$  on the Si surface perturbs the electronic structure of the molecule enough to red shift or blue shift the absorption spectrum by 1 to 3 nm (2 nm corresponds to  $\sim 0.05$  eV at 217 nm), the peaks of the vibrational band will be aligned with the bands of available photons. A red- or blue

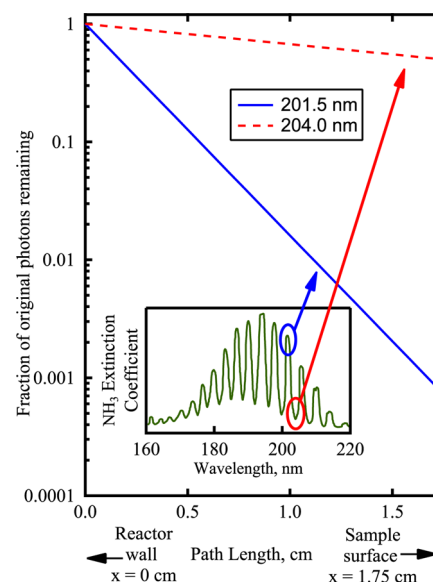


**Figure 7.** Beer–Lambert law was used to calculate the wavelength-dependent attenuation of UV photons by the  $\text{NH}_3$  ambient in the reactor with 10 Torr  $\text{NH}_3$  at 75 °C. At wavelengths corresponding to peaks in the absorption spectrum (inset), the photons are nearly all absorbed before reaching the sample (blue solid line), but at wavelengths corresponding to the valleys in the absorption spectrum, 50% of the original photons are available to drive photochemistry at the sample surface (red dashed line).  $\text{NH}_3$  absorbance spectrum from Okabe.<sup>11</sup> These calculations were done for the indirect configuration (no reflection from the sample surface).

shift in the absorption spectrum allows the photons that make it through the gas to the sample surface to activate the  $\text{NH}_3$  molecules there. Alternatively, broadening of the intense vibrational bands could also have the effect of increasing the likelihood that the physisorbed molecule would absorb available photons by increasing the absorption coefficient at those wavelengths corresponding to the valleys between the intense vibrational bands. Another possibility is that physisorption changes the molecular symmetry, enabling previously forbidden transitions.<sup>7</sup>

All of the  $\text{NH}_3$  excited states require the trigonal pyramidal  $\text{NH}_3$  ground state to transition to a planar configuration with the lone pair distributed above and below the molecular plane. When  $\text{NH}_3$  physisorbs with the N toward the substrate on a bare surface<sup>43</sup> or with the lone pair hydrogen-bonded to surface amine or hydride groups,<sup>46</sup> the electronic structure of the molecule is altered. The donation of electron density from the  $\text{NH}_3$  lone pair to the surface, either to Si–H groups or, more likely,  $-\text{NH}_2$  or  $-\text{OH}$ , would reduce the  $\text{sp}^3$  nature of the intramolecular bonds, giving the three N–H bonds more planar  $\text{sp}^2$  character. With the H atoms relaxed from the trigonal pyramid configuration toward the planar configuration, the energy barrier between the ground (pyramidal) and excited (planar) states would be lowered, resulting in a red shift. The stabilizing effect of the surface could be acting on either the ground or excited states. In other words, the surface could promote the reaction channel leading to a planar transition state either by elongating N–H bonds or accepting electron density from the N atom. Again, Figure 6 does show minimal N deposition at 225 and 230 nm, but this cannot be cited as evidence of a red shift because the monochromator was set for



high throughput, not high resolution, and transmitted some sub-220 nm photons even when centered at 230 nm.

Chen and Osgood<sup>10</sup> observed red shifts of the absorption spectrum for physisorbed  $\text{Cd}(\text{CH}_3)_2$  molecules on fused silica at 0 °C, and pressures between 1 and 4 Torr. The degree of red shift was not quantified by the authors, but inspection of the published spectra indicates the shift was between 1 and 2 nm and reportedly increased with pressure. In addition to the red shift, the vibrational features of the spectrum broadened and became indistinct. The  $\text{Cd}(\text{CH}_3)_2$  coverage on the silica surfaces was not quantified, but Chen and Osgood attributed the change in the absorbance spectrum to the formation of a liquid-like state for the physisorbed molecules where adsorbate–adsorbate interactions perturbed the spectrum. They additionally report the observation of an additional absorbance feature, forbidden in gas phase molecules, but active in the physisorbed layer that enables photodissociation at longer wavelengths than observed in the gas phase.<sup>7</sup> Similar results were observed for  $\text{Hg}(\text{CH}_3)_2$  and  $\text{Zn}(\text{CH}_3)_2$ .<sup>7</sup>

As described above, Chakarov and Ho<sup>9</sup> quantified the red shift in the  $\text{H}_2\text{S}$  absorbance spectrum at roughly 22 nm for molecules chemisorbed on Si(111). They also report a 10 nm red shift for  $\text{H}_2\text{S}$  condensed on Cu(111).<sup>47</sup> Because of the relatively large bandwidth of the monochromator (11 nm fwhm), we can't conclude that the red shift is 5 nm as the difference between the peaks of the  $\text{NH}_3$  absorption spectrum and N atom coverage envelope seem to imply. The  $\text{NH}_3$  absorbance red shift could be larger than 2 nm, but a large shift would imply a strong interaction between the surface and adsorbate, which was not expected for this system. Measuring the magnitude of the shift is important because it quantifies the strength of the interaction between the ground and excited states of a physisorbed molecule and a solid surface.

The deposition rate increased with increasing UV flux at 10 Torr, indicating the reaction rate was limited by the availability of photons within the necessary wavelength range. The deposition rate also increased with increasing  $\text{NH}_3$  pressure (increased  $\text{NH}_3$  flux) at a fixed UV flux, suggesting that the reaction was also limited by the availability of the physisorbed  $\text{NH}_3$  reactant. While the amount of physisorbed  $\text{NH}_3$  increased with increasing pressure, it also decreased with increasing temperature. If the reaction mechanism was limited by the availability of physisorbed  $\text{NH}_3$ , then the reaction rate would have been expected to decrease as the sample temperature was raised, particularly because the activation energy for this reaction was provided by the photons rather than thermally. Increasing the surface temperature from 25 to 150 °C, would be expected to decrease the population of physisorbed  $\text{NH}_3$  by roughly half, assuming the adsorption energy to be 0.15 eV,<sup>48</sup> but a strong temperature dependence was not observed (Figure 4). There was a possible increase in the deposition rate as the temperature was increased from 25 to 75 °C, but the repeatability of the 25 °C, data was too low to make a definitive conclusion.

There have been many scanning tunneling microscopy (STM) studies and density functional theory (DFT) calculations modeling the chemisorption of  $\text{NH}_3$  on the bare Si(100)-2×1 surface,<sup>49</sup> but there is a lack of work investigating how  $\text{NH}_3$  interacts with H-terminated Si(100) surfaces. Recent work has looked at interactions between gas phase  $\text{NH}_3$  molecules and ideal Si(100)-2×1 surfaces terminated with dissociatively chemisorbed ammonia ( $\text{H}-\text{Si}-\text{Si}-\text{NH}_2$ ), including experimental evidence for hydrogen bonding between the

physisorbed and chemisorbed  $\text{NH}_3$ .<sup>49,50</sup> DFT calculations have put the adsorption energy for  $\text{NH}_3$  on a primary amine ( $\text{Si}-\text{NH}_2$ ) at ~0.3 eV (2.0 Å bond length) and at ~0.09 eV (2.8 Å bond length) for  $\text{NH}_3$  on a hydride ( $\text{Si}-\text{H}$ ) adjacent to a primary amine.<sup>46</sup> For this reason, the population of physisorbed  $\text{NH}_3$  should be expected to increase as the population of surface amines increases. The hydrogen bonding is stronger when it is between the lone pair on the physisorbed molecule and the H atom of the chemisorbed amine as the surface withdraws some electron density, leaving the chemisorbed amine slightly positive.<sup>49</sup> Surface oxygen or hydroxyl groups are also expected to promote physisorption of  $\text{NH}_3$ . Even if the initial coverage of physisorbed  $\text{NH}_3$  was low and temperature dependent, the coverage of physisorbed  $\text{NH}_3$  would be expected to increase as the surface amine coverage increased and provided more sites for gas phase  $\text{NH}_3$  to hydrogen bond. Because the hydrogen bonds are more stable than the physisorption energy predicted by Picaud and Girardet,<sup>48,51</sup> the coverage would be less dependent on temperature between 25 and 150 °C. If, however, there was a significant increase in the population of adsorbed  $\text{NH}_3$  during the course of the reaction due to increased hydrogen bonding, then the reaction curves in Figure 3 would have shown an inflection point as evidence of this autocatalytic effect. The effect was not observed, indicating the population of adsorbed  $\text{NH}_3$  was not strongly influenced by reaction progress.

Even with the photon-activated rate limiting step ( $\text{NH}_3$  dissociation), there may still be thermally activated steps in the reaction mechanism, such as  $\text{NH}_2^\bullet$  radical abstracting a hydrogen atom from the Si surface. The competing effects of thermally activated reaction steps in parallel with the inverse temperature dependence expected for physisorption could compensate as the temperature was increased. Moreover, the density of gas in the reactor decreased by ~35% and the  $\text{NH}_3$  flux decreased by ~17% when the temperature was raised from 25 to 150 °C. Decreasing gas density would have reduced photon attenuation, allowing more photons to reach the sample surface, but decreasing flux would have reduced the population of physisorbed  $\text{NH}_3$  available for reaction.

Mellqvist and Rosen<sup>52</sup> measured the UV absorption spectrum of  $\text{NH}_3$  at 25 and 405 °C, finding that the vibrational features broadened and shortened such that there was a negligible effect on the integrated absorption cross section, but the cross section at any specific wavelength could increase or decrease with temperature. If the enhanced amine deposition rate in the direct geometry was due to a red or blue shift in the absorbance spectrum, the broadening of the vibrational features with increasing temperature could decrease the magnitude of the enhancement. Two additional absorption bands have been observed in the  $\text{NH}_3$  spectrum at wavelengths longer than 220 nm. These hot bands have been observed at pressures greater than 15 Torr,<sup>53</sup> or temperatures greater than 150 °C.<sup>52</sup> Because these hot bands correspond to wavelengths with plentiful photons, this effect could potentially offset the decreased deposition rate expected at higher temperatures due to a lower population of physisorbed reactant molecules.

The H-terminated starting surface was stable against oxidation, experiencing only minimal oxidation after several hours, and even up to several days, in atmosphere.<sup>54</sup> The amine terminated surface, however, was significantly more reactive toward water, becoming measurably oxidized by the low concentration of water present in the source  $\text{NH}_3$  gas—the surface amines apparently catalyzed the oxidation of Si by  $\text{H}_2\text{O}$ .

Klaus and George<sup>55</sup> used  $\text{NH}_3$  as a catalyst to promote  $\text{SiO}_2$  deposition by ALD using  $\text{SiCl}_4$  and  $\text{H}_2\text{O}$  as precursors and proposed two potential mechanisms by which  $\text{NH}_3$  could catalytically participate in the reaction: (1) hydrogen bonding between N of  $\text{NH}_3$  and H of  $\text{H}_2\text{O}$  would make the O more nucleophilic and more likely to bond with Si, or (2)  $\text{NH}_3$  could act as a nucleophile and attack the Si of  $\text{SiCl}_4$  to form a pentacoordinated Si complex that is more susceptible to attack by  $\text{H}_2\text{O}$ . Mechanism 1 is more plausible for the aminated surfaces produced in this work as the Si on the surface is not as electron deficient as the Si of  $\text{SiCl}_4$ , and the activated Si would be more likely to encounter another  $\text{NH}_3$  molecule rather than a scarce  $\text{H}_2\text{O}$  molecule. Similar work using pyridine as a catalyst also supports the first mechanism as the most likely.<sup>56</sup> Because the aminated surfaces were still highly susceptible to oxidation even after the  $\text{NH}_3$  reactant had been purged, it is evident that the surface amines had a catalytic effect, rather than the result of gas phase  $\text{NH}_3$  molecules. Another possibility is that the amine, being anchored to the surface, provided a hydrogen bonding site for  $\text{H}_2\text{O}$  in close proximity to the Si and increased the odds of the oxygen reacting with a Si atom made electron deficient by the Si–N bond. Because O has a higher electronegativity than N and forms a stronger bond with Si (800 kJ/mol for Si–O versus 437 kJ/mol for Si–N),<sup>57</sup> once  $\text{H}_2\text{O}$  was able to replace a surface amine with O, the replacement was permanent.

## CONCLUSIONS

UV light was used to activate  $\text{NH}_3$  molecules, generating  $\text{NH}_2^\bullet$  radicals that replaced the H-termination on Si(100) with N in the form of amine groups. When the light was parallel to the Si surface, only photodissociation of  $\text{NH}_3$  molecules and diffusion of the fragments could produce deposition. The N coverage reached a maximum at conditions where the density of ammonia gas balanced the fluence of light. When the light was incident on the Si surface, gas phase photodissociation and diffusion still contributed but was a minor pathway compared to photodissociation of  $\text{NH}_3$  molecules physisorbed on the Si surface. The N coverage increased monotonically with  $\text{NH}_3$  partial pressure up to 100 Torr, the highest pressure studied. The Si surface atoms interacted with physisorbed  $\text{NH}_3$  molecules altering their electronic structure and increasing the photodissociation cross-section at the wavelengths where photons were not fully attenuated by the gas phase. This surface-enhanced direct excitation mechanism occurs because of either a red shift or blue shift in the absorption spectrum or a broadening of the intense vibrational bands within the spectrum. Experiments with monochromatic light perpendicular to the surface demonstrated that the photon energy required for deposition was close in energy to that for gas phase dissociation, indicating that the same photodissociation mechanism applied to both conditions. Also supporting direct photon absorption as the mechanism is the lack of any resonant energy levels on  $\text{NH}_3$  to which an electron could attach, as required by a mechanism driven by a hot electron produced photochemically from the surface. Because the deposition reaction is photon initiated, the reaction did not show a strong temperature dependence. The surface was not etched by the photodissociated ammonia fragments at 75 °C because the surface roughness was the same as an H-terminated surface. The surface amines catalyzed the oxidation of Si by  $\text{H}_2\text{O}$ , which was a common contaminant on the postdeposition surfaces. Because the N deposition reaction increased with increasing

UV flux and the oxidation reaction did not, the N coverage saturated at a higher coverage when more intense illumination was used. On the basis of the total coverage of N and O achieved ( $\sim 1.8$  N atoms per Si surface atom), some of the deposited amine and oxide groups were incorporated in the Si surface atom back-bonds. Oxidation is undesirable for production of microelectronic devices, but eliminating water from the gas stream should solve this problem. The results show that the electronic structure of molecules that associate even weakly with surfaces, in this case via hydrogen-bonding, is perturbed enough to have a dramatic impact on photochemical reactions. This idea could find application in catalysis, thin film growth, and electrochemistry.

## ASSOCIATED CONTENT

### Supporting Information

Description of XPS coverage calibration, the model for the production rate of  $\text{NH}_2^\bullet$  radicals, the rate of electron–hole pair generation, the energetics of Si and  $\text{NH}_3$ , and the reaction mechanism for N deposition. This material is available free of charge via the Internet at <http://pubs.acs.org/>.

## AUTHOR INFORMATION

### Corresponding Author

\*A. J. Muscat: e-mail, [muscat@erc.arizona.edu](mailto:muscat@erc.arizona.edu); tel, +1(520) 626-6580.

### Notes

The authors declare no competing financial interest.

## ACKNOWLEDGMENTS

Funding was provided by NSF. We thank Adam Thorsness for the graphic used in the TOC entry.

## REFERENCES

- (1) Finstad, C. C.; Thorsness, A. G.; Muscat, A. J. The Mechanism of Amine Formation on Si(100) Activated with Chlorine Atoms. *Surf. Sci.* **2006**, *600*, 3363–3374.
- (2) Terry, J.; MO, R.; Wigren, C.; Cao, R.; Mount, G.; Pianetta, P.; Linford, M. R.; Chidsey, C. E. Reactivity of the H-Si(111) Surface. *Nucl. Instrum. Methods Phys. Res., Sect. B* **1997**, *133*, 94–101.
- (3) Gluck, N. S.; Ying, Z.; Bartosch, C. E.; Ho, W. Mechanisms of Laser Interaction with Metal Carbonyls Adsorbed on Si(111)7×7: Thermal vs Photoelectronic Effects. *J. Chem. Phys.* **1987**, *86*, 4957–4978.
- (4) Zhu, X.-Y.; Wolf, M.; Huett, T.; White, J. M. Laser-Induced Interaction of Ammonia with GaAs(100). I. Dissociation and Nitridation. *J. Chem. Phys.* **1992**, *97*, 5856–5867.
- (5) Zhu, X.-Y.; Wolf, M.; Huett, T.; White, J. M. Laser-Induced Interaction of Ammonia with GaAs(100). II. Dissociation and Nitridation. *J. Chem. Phys.* **1992**, *97*, 5868–5875.
- (6) Sun, Y.-M.; Huett, T.; Sloan, D.; White, J. M. Nonthermally Driven Surface Chemistry of Phosphine on GaAs(100). *J. Vac. Sci. Technol. A* **1994**, *12*, 2287–2292.
- (7) Chen, C. J.; Osgood, R. M. Surface-Catalyzed Photochemical Reactions of Physisorbed Molecules. *Appl. Phys. A: Mater. Sci. Process.* **1983**, *31*, 171–182.
- (8) Zhou, X.-L.; Zhu, X.-Y.; White, J. Photochemistry at Adsorbate/Metal Interfaces. *Surf. Sci. Rep.* **1991**, *13*, 73–220.
- (9) Chakarov, D.; Ho, W. Thermal and Photo-Induced Desorption, Dissociation, Reactions of  $\text{H}_2\text{S}$  Adsorbed on Si(111)-7×7. *Surf. Sci.* **1995**, *323*, 57–70.
- (10) Chen, C. J.; Osgood, R. M., Jr. *Spectroscopy and Photoreactions of Organometallic Molecules on Surfaces. Laser Diagnostics and Photochemical Processing for Semiconductor Devices*; Materials Research

Society Symposia Proceedings, Vol. 17; MRS: New York, Amsterdam, Oxford, 1983; pp 169–175.

(11) Okabe, H. *Photochemistry of Small Molecules*, 1st ed.; John Wiley & Sons, Inc.: New York, Chichester, Brisbane, Toronto, 1978.

(12) Runau, R.; Peyerimhoff, S. D.; Buenker, R. J. Ab Initio Study of the Photodissociation of Ammonia. *J. Mol. Spectrosc.* **1977**, *68*, 253–268.

(13) Schurath, U.; Tiedemann, P.; Schindler, R. N. The Photolysis of Ammonia at 2062 Å in the Presence of Ethylene. *J. Phys. Chem.* **1969**, *73*, 456–459.

(14) Bach, A.; Hutchison, J. M.; Holiday, R. J.; Crim, F. F. Competition Between Adiabatic and Nonadiabatic Pathways in the Photodissociation of Vibrationally Excited Ammonia. *J. Phys. Chem. A* **2003**, *107*, 10490–10496.

(15) Hudson, R. D. Critical Review of Ultraviolet Photoabsorption Cross Sections for Molecules of Astrophysical and Aeronomic Interest. *Rev. Geophys. Space Phys.* **1971**, *9*, 305–406.

(16) Wells, K. L.; Perriam, G.; Stavros, V. G. Time-Resolved Velocity Map Ion Imaging Study of NH<sub>3</sub> Photodissociation. *J. Chem. Phys.* **2009**, *130*, 074308.

(17) Zhou, X.-L.; Flores, C. R.; White, J. M. Decomposition of NH<sub>3</sub> on Si(100): a SSIMS Study. *Surf. Sci. Lett.* **1992**, *268*, L267–L273.

(18) Widjaja, Y.; Musgrave, C. B. Ab Initio Study of the Initial Growth Mechanism of Silicon Nitride on Si(100)-(2×1) using NH<sub>3</sub>. *Phys. Rev. B* **2001**, *64*, 205303.

(19) Xu, X.; Kang, S.-Y.; Yamabe, T. Nitridation of Si(100)-(2×1) Surface by NH<sub>3</sub>: A Quantum Chemical Cluster Model Study. *Phys. Rev. Lett.* **2002**, *88*, 076106.

(20) Dabrowski, J.; Mussig, H.-J. *Silicon Surfaces and Formation of Interfaces: Basic Science in the Industrial World*; World Scientific Publishing Co. Pte. Ltd.: Singapore, 2000.

(21) Kim, J. W.; Yeom, H. W. Thermal Decomposition of NH<sub>3</sub> on the Si(100) Surface. *Surf. Sci. Lett.* **2003**, *546*, L820–828.

(22) Kubler, L.; Bischoff, J. L.; Bolmont, D. General Comparison of the Surface Processes Involved in the Nitridation of Si(100)-2×1 by NH<sub>3</sub> and in SiN Film Deposition: A Photoemission Study. *Phys. Rev. B* **1988**, *38*, 13113–13123.

(23) Guizot, J.-L.; Alnot, P.; Wyczisk, F.; Perrin, J.; Allain, B. Kinetics of Deposition and Electrical Properties of Silicon Nitride Films Obtained by 185 nm Photolysis of SiH<sub>4</sub>-NH<sub>3</sub> Mixtures. *Semicond. Sci. Technol.* **1991**, *6*, 582–589.

(24) Watanabe, T.; Ichikawa, A.; Sakuraba, M.; Matsuura, T.; Murota, J. Atomic-Order Thermal Nitridation of Silicon at Low Temperatures. *J. Electrochem. Soc.* **1998**, *145*, 4252–4256.

(25) Dai, M.; Wang, Y.; Kwon, J.; Halls, M. D.; Chabal, Y. J. Nitrogen Interaction with Hydrogen-Terminated Silicon Surfaces at the Atomic Scale. *Nat. Mater.* **2009**, *8*, 825–830.

(26) Bater, C.; Sanders, M.; Craig, J. H., Jr. Ammonia as a Precursor in Electron-Enhanced Nitridation of Si(100). *Surf. Interface Anal.* **2000**, *29*, 208–214.

(27) Cerrina, F.; Lai, B.; Wells, G. M.; Wiley, J. R.; Kilday, D. G.; Margaritondo, G. Synchrotron-Radiation-Induced Surface Nitridation of Silicon at Room Temperature. *Appl. Phys. Lett.* **1987**, *50*, 533–534.

(28) Sugii, T.; Ito, T.; Ishikawa, H. Excimer Laser Enhanced Nitridation of Silicon Substrates. *Appl. Phys. Lett.* **1984**, *45*, 966–968.

(29) Watanabe, T.; Sakuraba, M.; Matsuura, T.; Murota, J. Atomic-Order Thermal Nitridation of Si(100) and Subsequent Growth of Si. *J. Vac. Sci. Technol. A* **2001**, *19*, 1907–1911.

(30) Perrine, K. A.; Teplyakov, A. V. Reactivity of Selectively Terminated Single Crystal Silicon Surfaces. *Chem. Soc. Rev.* **2010**, *39*, 3256–3274.

(31) Rodriguez-Reyes, J. C. F.; Teplyakov, A. V. Surface Transamination Reaction for Tetrakis(dimethylamido)titanium with NH<sub>x</sub>-Terminated Si(100) Surfaces. *J. Phys. Chem. C* **2007**, *111*, 16498–16505.

(32) Maikap, S.; Lee, J.-H.; Mahapatra, R.; Pal, S.; No, Y.; Choi, W.-K.; Ray, S.; Kim, D.-Y. Effects of Interfacial NH<sub>3</sub>/N<sub>2</sub>O-Plasma Treatment on the Structural and Electrical Properties of Ultra-Thin

HfO<sub>2</sub> Gate Dielectrics on p-Si Substrates. *Solid State Electron.* **2005**, *49*, 524–528.

(33) Triyoso, D. H.; Hegde, R. I.; Grant, J.; Fejes, P.; Liu, R.; Roan, D.; Ramon, M.; Werho, D.; Rai, R.; La, L. B.; et al. Film Properties of ALD HfO<sub>2</sub> and La<sub>2</sub>O<sub>3</sub> Gate Dielectrics Grown on Si with Various Pre-deposition Treatments. *J. Vac. Sci. Technol. B* **2004**, *22*, 2121–2128.

(34) Gardener, J.; Owen, J. H. G.; Miki, K.; Heutz, S. A scanning Tunneling Microscopy Investigation into the Initial Stages of Copper Phthalocyanine Growth on Passivated Silicon Surfaces. *Surf. Sci.* **2008**, *602*, 843–851.

(35) Kim, K. H.; Watanabe, K.; Menzel, D.; Freund, H.-J. UV Photo-Dissociation and Photodesorption of N<sub>2</sub>O on Ag(111). *J. Phys.: Condens. Matter* **2010**, *22*, 084012.

(36) Finstad, C. C.; Montano-Miranda, G.; Thorsness, A. G.; Muscat, A. J. Gas Phase Preparation and Analysis of Semiconductor Surfaces in a Clustered Reactor Apparatus. *Rev. Sci. Instrum.* **2006**, *77*, 093907.

(37) Wagner, C. D. Sensitivity Factors for XPS Analysis of Surface Atoms. *J. Electron Spectrosc. Relat. Phenom.* **1983**, *32*, 99–102.

(38) O'Hanlon, J. F. *A User's Guide to Vacuum Technology*, 2nd ed.; John Wiley & Sons, Inc.: New York, Chichester, Brisbane, Toronto, Singapore, 1989.

(39) National Institute of Standards and Technology, NIST X-ray Photoelectron Spectroscopy Database. <http://srdata.nist.gov/xps/>, Accessed on May 20, 2013.

(40) Aspnes, D.; Studna, A. Dielectric Functions and Optical Parameters of Si, Ge, GaP, GaSb, InP, InAs, and InSb from 1.5 to 6.0 eV. *Phys. Rev. B* **1983**, *27*, 985.

(41) Ying, Z.; Ho, W. Photogenerated-Charge-Carrier-induced Surface Reactions: NO on Si(111) 7×7. *Phys. Rev. Lett.* **1988**, *60*, 57.

(42) Pickering, C.; Hodge, A. M.; Daw, A. C.; Robbins, D. J.; Pearson, P. J.; Greef, R. Interpretation of UV Reflectance Measurements on Silicon-on-Sapphire by Spectral Reflectance and Spectroscopic Ellipsometry Studies. Materials Research Society Symposia Proceedings, Volume 53: Semiconductor-on-Insulator and Thin Film Transistor Technology. Pittsburgh, Pa, 1986; pp 317–322.

(43) Hasselbrink, E. In *Handbook of Surface Science*; Hasselbrink, E., Lundqvist, B. I., Eds.; Elsevier: Amsterdam, 2008; Vol. 3, pp 621–679.

(44) Sze, S. M. *Physics of Semiconductor Devices*, 2nd ed.; John Wiley & Sons, Inc.: New York, Chichester, Brisbane, Toronto, Singapore, 1981.

(45) Alderdice, D. S. Electronic Spectra of Transition Metal Complexes: Part I. *J. Mol. Spectrosc.* **1965**, *15*, 509–520.

(46) Kim, Y.-S.; Koo, J.-Y.; Kim, H. Adsorption States of the Self-assembly of NH<sub>3</sub> Molecules on the Si(001) Surface. *J. Phys.: Condens. Matter* **2009**, *21*, 064237.

(47) Chakarav, D.; Ho, W. Enhancement of Photoyield Associated with Disruption of Bonding During Adsorbate Sublimation. *Surf. Sci. Lett.* **1991**, *258*, L691–L696.

(48) Picaud, S.; Girardet, C. Molecular Physisorption on Atom-Adsorbed Unreconstructed (111) Silicon Surfaces. *Surf. Sci.* **1991**, *258*, 210–224.

(49) Owen, J. H. G. Competing Interactions in Molecular Adsorption: NH<sub>3</sub> on Si(001). *J. Phys.: Condens. Matter* **2009**, *21*, 443001.

(50) Owen, J. H. G.; Bowler, D. R. The Origin of Inter-Dimer-Row Correlated Adsorption for NH<sub>3</sub> on Si(001). *Surf. Sci.* **2009**, *603*, 2902–2906.

(51) Picaud, S.; Ramseyer, C.; Hoang, P. N. M.; Girardet, C. Ammonia and Water Physisorption on a H-Passivated Si(111) Surface: A Study of Admolecule Motions. *Surf. Sci.* **1992**, *272*, 172–181.

(52) Mellqvist, J.; Rosen, A. DOAS for Flue Gas Monitoring—I. Temperature Effects in the U.V./Visible Absorption Spectra of NO, NO<sub>2</sub>, SO<sub>2</sub> and NH<sub>3</sub>. *J. Quant. Spectrosc. Radiat. Transfer* **1996**, *56*, 187–208.

(53) Saraswathy, P.; Sunanda, K.; Aparna, S.; Sekhar, B. N. R. Photoabsorption Spectra of Ammonia in 1050 to 2250 Angstrom Region. *Spectrosc. Lett.* **2010**, *43*, 290–297.

(54) Bender, H.; Verhaverbeke, S.; Heyns, M. M. Hydrogen Passivation of HF-Last Cleaned (100) Silicon Surfaces Investigated

by Multiple Internal Reflection Infrared Spectroscopy. *J. Electrochem. Soc.* **1994**, *141*, 3128–3136.

(55) Klaus, J. W.; George, S. M. SiO<sub>2</sub> Chemical Vapor Deposition at Room Temperature Using SiCl<sub>4</sub> and H<sub>2</sub>O with an NH<sub>3</sub> Catalyst. *J. Electrochem. Soc.* **2000**, *147*, 2658–2664.

(56) Du, Y.; Du, X.; George, S. M. Mechanism of Pyridine-Catalyzed SiO<sub>2</sub> Atomic Layer Deposition Studied by Fourier Transform Infrared Spectroscopy. *J. Phys. Chem. C* **2007**, *111*, 219–226.

(57) Luo, Y.-R. *Bond Dissociation Energies*, 91st ed.; CRC Handbook of Chemistry and Physics; CRC Press: Cleveland, OH, 2010; Chapter 9, pp 9-65 to 9-70.